(Received 10 March 2025, Accepted 25 April 2025, Scheduled 6 May 2025)

High Isolation mm-Wave 8-Element MIMO Antenna for 5G Applications

Nayera Nahvi* and Khalid Muzaffar

Department of Electronics and Communication Engineering, Islamic University of Science and Technology, Awantipur, J&K, India

ABSTRACT: The present study describes the architecture of a defected ground structure (DGS)-based eight-element multiple-input multiple-output (MIMO) antenna. It functions in the millimeter-wave spectrum n258 (24.25–27.5 GHz) and is mainly intended for fifth-generation (5G) applications. Each antenna element has an elliptical slot at the ground plane and a hook-shaped antenna integrated into it to reduce the mutual coupling among the adjacent antenna elements. With a wide bandwidth of 5 GHz and an isolation level greater than 37 dB, the proposed antenna effectively covers the frequency range of 22.5 to 27.5 GHz. At the designated resonant frequency, it generates a directed radiation pattern and gain of 6.31 dBi. The proposed antenna's diversity system performance characteristics are assessed using metrics like channel capacity loss (CCL), diversity gain (DG), mean effective gain (MEG), and envelope correlation coefficient (ECC). The 8-port proposed MIMO antenna prototype, exhibiting overall dimensions of $62.7 \times 31 \times 0.787\,\text{mm}^3$, has been constructed utilizing an economical FR4 substrate, demonstrating a substantial association between the computed and measured outcomes, thereby establishing its viability as a potential candidate for 5G communications.

1. INTRODUCTION

In the rapidly evolving area of wireless communication technology, high data transfer speeds are desirable. However, because of the growing user base, there are issues regarding congestion on the available wireless spectrum. The potential of the 5G mobile network transition is far higher than that of the 4G systems. A key element of this transition is using millimeter-wave (mm-wave) frequencies, which hold immense promise for 5G applications [1]. Although mm-wave frequencies offer numerous benefits, they have drawbacks, such as atmospheric absorption, signal fading, and path loss attenuation [2]. These issues get more severe, mainly when we use a single antenna. As a result, the researchers were led to deal with atmospheric absorptions at mm-wave frequencies by utilizing MIMO capabilities. Also, the spectrum efficiency, data rates, channel capacity, and link reliability are increased using the MIMO technique [3]. There are specific challenges in assembling many antenna elements in a MIMO arrangement. Improving MIMO antenna element isolation is one approach to enhance the wireless system's overall performance [4, 5].

It is very challenging to design compact MIMO antennas. The efficiency of the system is drastically affected by the inevitable mutual coupling effect due to the close spacing of antennas. Thus, the addressal of this issue is incredibly significant [6, 7]. Several techniques exist in the literature for isolation enhancement and mutual coupling reduction, such as decoupling networks [8], frequency selective surfaces (FSS) [9], electromagnetic band gap (EBG) [10], split ring resonator (SRR) [11], metamaterials [12], and absorbers [13]. Numerous challenges in terms of design complexity arise when these structures are integrated. In [14], using the decoupling structure, a MIMO antenna design operating at 28 GHz attains an isolation of -30 dB. The dual-element antenna design shows a considerable reduction in mutual coupling by placing a single-column Electromagnetic Bandgap (EBG) structure and a ground stub between the two radiating patches [15]. To increase isolation, a Defected Ground Structure (DGS) based quad-port circularly polarized MIMO antenna in [16] uses circular parasitic structures forming the decoupling structure. In [17], a metamaterial-based antenna design with improved isolation is introduced. A dual-element circularly polarised MIMO antenna in [18] achieves isolation optimization using different antenna orientations. An ultra-wideband, compact antenna design operating at 26 GHz is presented in [19]. CSRR and DGS are used in a low-profile, compact antenna of two rectangular patches connected by a corporate feed network for better isolation [20]. In [21], a MIMO antenna consisting of two crescent-shaped patches, operating at triple bands and having slotted ground, is presented. Ref. [22] proposed a 4-port compact monopole patch antenna operating at 26 GHz. For impedance bandwidth optimization, circular and rectangular slots were etched in the ground. Also, semi-circular slots etched on the edges improved the isolation. Ref. [23] introduced a dual-element MIMO antenna design using a tapered microstrip feed line for bandwidth widening.

The antenna designs discussed above adopted different techniques for isolation improvement. Most of them tend to have complex designs. The complex configurations pose significant difficulties in precise fabrication, particularly at reduced dimensions, resulting in possible inaccuracies and discrepan-

* Corresponding author: Nayera Nahvi (nayera.nahvi@iust.ac.in).

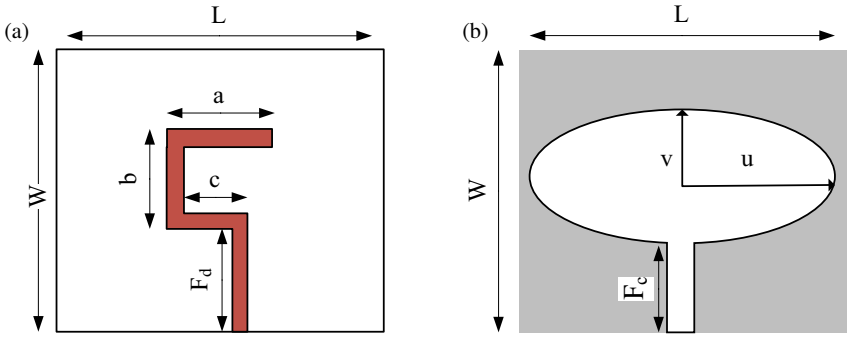

FIGURE 1. (a) Front view. (b) Rear view of single-element antenna.

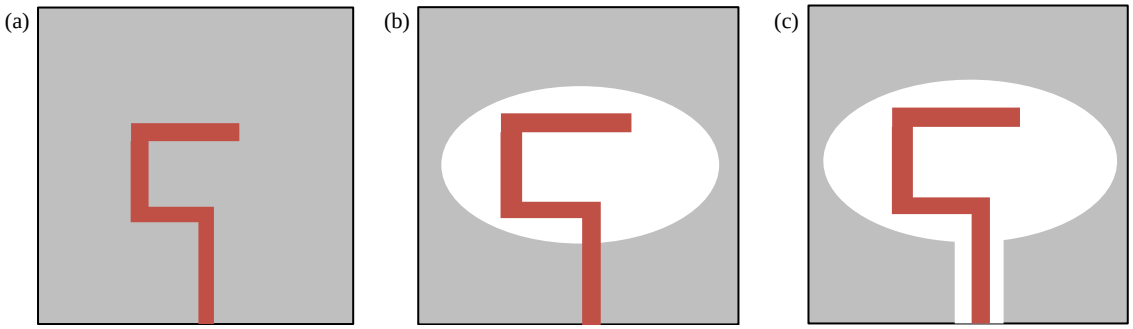

FIGURE 2. Single-element antenna progression steps. (a) Antenna 1 (with the entire ground plane). (b) Antenna 2 (with slot). (c) Antenna 3 (proposed).

cies. Also, some designs suffer from low isolation, low gain, and reduced operating bandwidth.

This work describes a slotted ground plane, highly isolated, 8-element MIMO antenna with acceptable gain over a wide operating bandwidth without any decoupling structure.

2. ANTENNA DESIGN

2.1. Design Methodology for Single Element Antenna

With a thickness of 0.787 mm and a dielectric constant of 4.4, an FR-4 substrate is used for fabricating the antenna's hook-shaped radiator. The dimensions and configuration of the designed single-element MIMO antenna are shown in Fig. 1. The design's front and back views are shown in Figs. 1(a) and (b). Table 1 displays the optimal layout parameters of the designed single-element MIMO antenna configuration.

TABLE 1. Optimized design values of the proposed individual antenna element.

Optimized Parameter	Value (mm)	Optimized Parameter	Value (mm)
L	16	W	16
a	6.5	F_d	6.5
b	5	F_c	5.5
c	7.5	L_f	1.4
u	6.2	v	4.45

Figure 2 delineates the progression steps of the individual element antenna architecture, culminating in the proposed design configuration. The initial design, as shown in Fig. 2(a), features a hook-shaped radiator and a complete ground plane.

The simulation results, shown in Fig. 3, indicate that the reflection coefficient (S_{11}) remains below -10 dB within a limited frequency range (22.5 GHz to 23.3 GHz), indicating inadequate impedance matching and a limited operational bandwidth. As illustrated in Fig. 2(b), a slot, elliptical in shape, has been created in the ground plane for improving the impedance

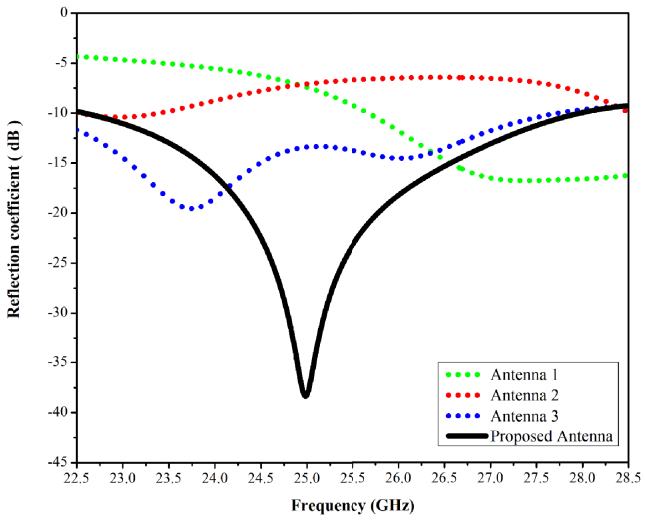

FIGURE 3. S_{11} for proposed single-element antenna.

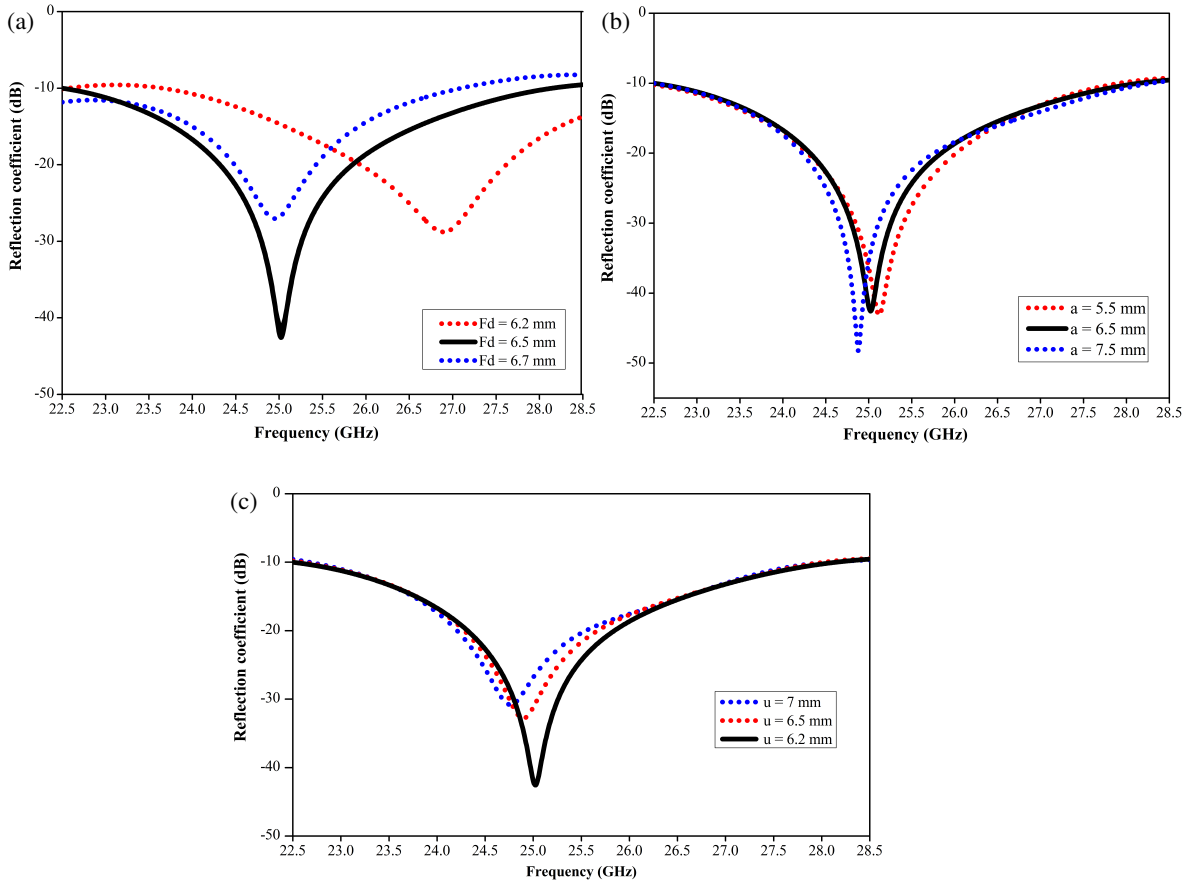

FIGURE 4. S_{11} of single element antenna for different values of (a) feed length (F_d); (b) stub length (a); (c) primary axis length of the ellipse (u).

matching and enhancing the operational bandwidth. Integrating the elliptical slot significantly enhances overall performance by mitigating mutual coupling and improving the frequency response characteristics.

The proposed configuration incorporates both the elliptical slot and a rectangular DGS, arranged with utmost care and optimized to enhance the performance, as shown in Fig. 2(c). With the reflection coefficient remaining below -10 dB, this configuration successfully attains the targeted frequency range (22.5–27.5 GHz), as shown in Fig. 3. The synergistic effect of the slot and rectangular DGS structures yields improved impedance matching and wide operational bandwidth. This sequential design advancement highlights the efficacy of incorporating DGS elements to attain the specified frequency range, enhanced isolation, and optimized performance tailored for millimeter-wave 5G applications.

2.2. Parametric Analysis

The attributes of the proposed single-element antenna design are strongly influenced by several design parameters. To ascertain the optimal values for these parameters, a parametric analysis is performed. Fig. 4 shows the antenna's S_{11} parameter for various values of these core design parameters.

The feed line length (F_d) is one of the essential parameters affecting the antenna's performance. As illustrated in Fig. 4(a), slight variations in the feed length (F_d) affect the impedance matching. Decreasing the values from 6.7 mm to 6.5 mm enhances the reflection coefficient (S_{11}) from -27 dB to -45 dB, improving the impedance matching.

The stub length (a) is another important factor to be taken into account. The simulated values of S_{11} as a function of changes in stub length are shown in Fig. 4(b). At $a = 6.5$ mm, the ideal results are achieved. The principal axis length of the elliptical slot (u) influences both the reflection coefficient (S_{11}) and the frequency of operation. It has a major impact on the mutual coupling and the suppression of surface currents. The resonant frequency shifts toward a higher frequency when u decreases, as shown in Fig. 4(c).

3. PROPOSED MIMO ANTENNA DESIGN

The single antenna is transformed into an eight-element MIMO antenna by placing the antennas adjacent to each other and opposite to each other. Elliptical and rectangular slots are created out of the ground plane to reduce the mutual coupling effect and bandwidth enhancement. The structure's entire dimensions are $62.7 \times 31\,\text{mm}^2$. Fig. 5 depicts the configuration of the sug-

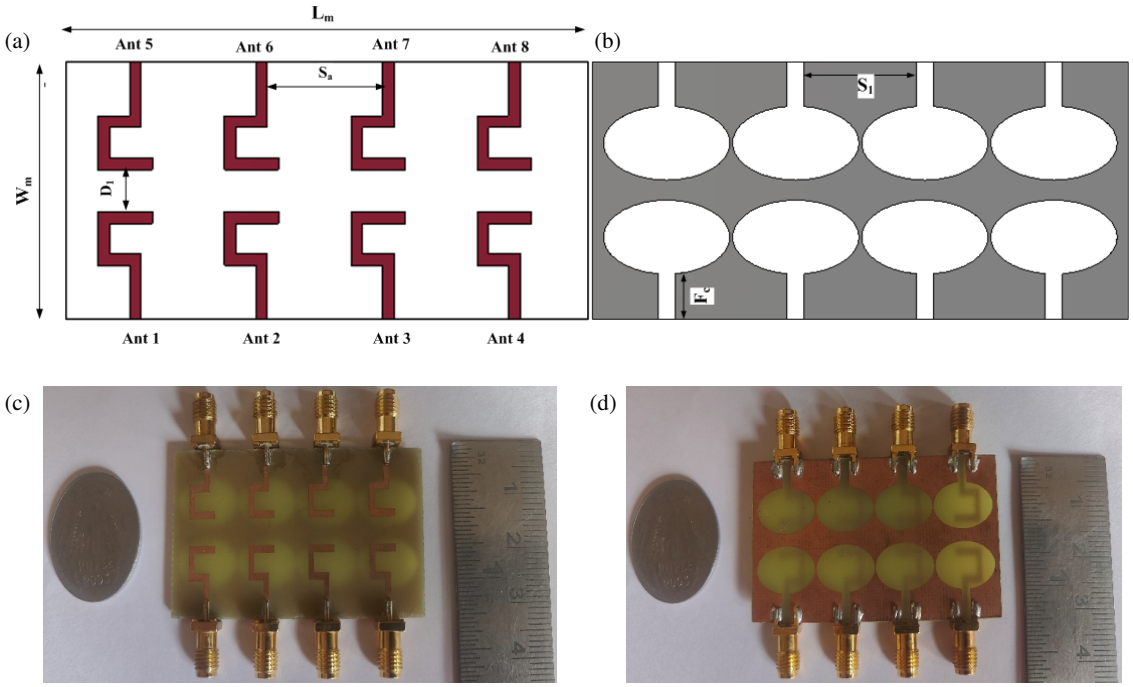

FIGURE 5. Proposed MIMO antenna design configuration. (a) Front view. (b) Rear view (with DGS). (c) Fabricated specimen (front view). (d) Fabricated specimen (back view).

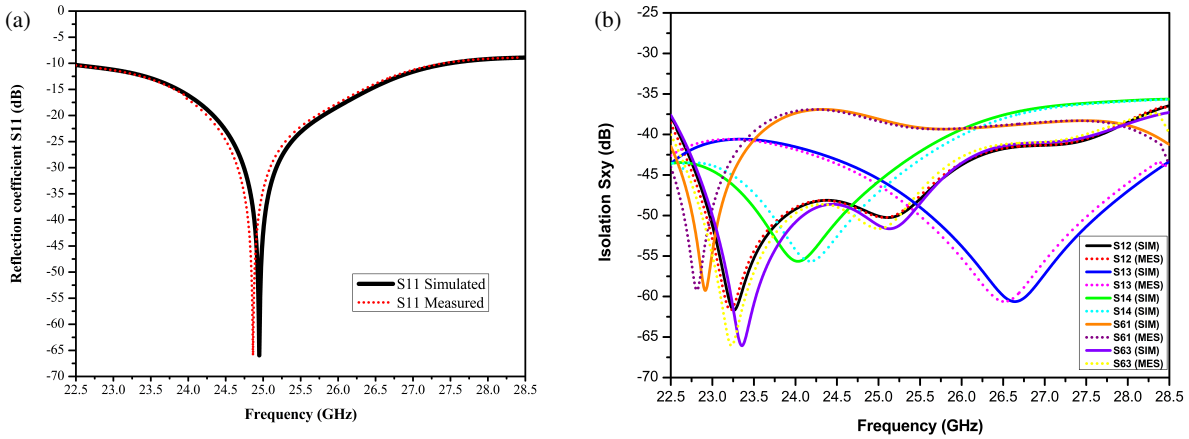

FIGURE 6. (a) Simulated and measured S_{11}. (b) Simulated and measured isolation (S_{XY}).

TABLE 2. Proposed MIMO antenna's design values.

Optimized Parameter	Value (mm)	Optimized Parameter	Value (mm)
L_m	62.7	W_m	31
D_1	5	S_1	13

gested MIMO antenna, and Table 2 lists its ideal dimensions.

4. RESULTS AND DISCUSSION

The computed and S-parameters measured for the proposed MIMO antenna are displayed in Fig. 6(a). The reflection coefficient is less than -10 dB throughout the whole operating bandwidth.

The simulations have been done using the CST (Computer Simulation Technology) Studio Suite. One port is energized during the experimental measurements, while the other ports are terminated with an impedance matching load of 50 Ω. Fig. 6(b) shows the isolation (S_{12}, S_{13}, S_{14}, S_{61}, and S_{63}) of the MIMO antenna design that has been proposed.

Due to its proximity to densely arranged antennas deployed in various orientations, including side-by-side and diagonal, port 1 is selected as the excitation port. Over the whole bandwidth, and the isolation is less than 37 dB. The possible human errors and tolerances in the fabrication process are accountable for the differences between simulated and measured values.

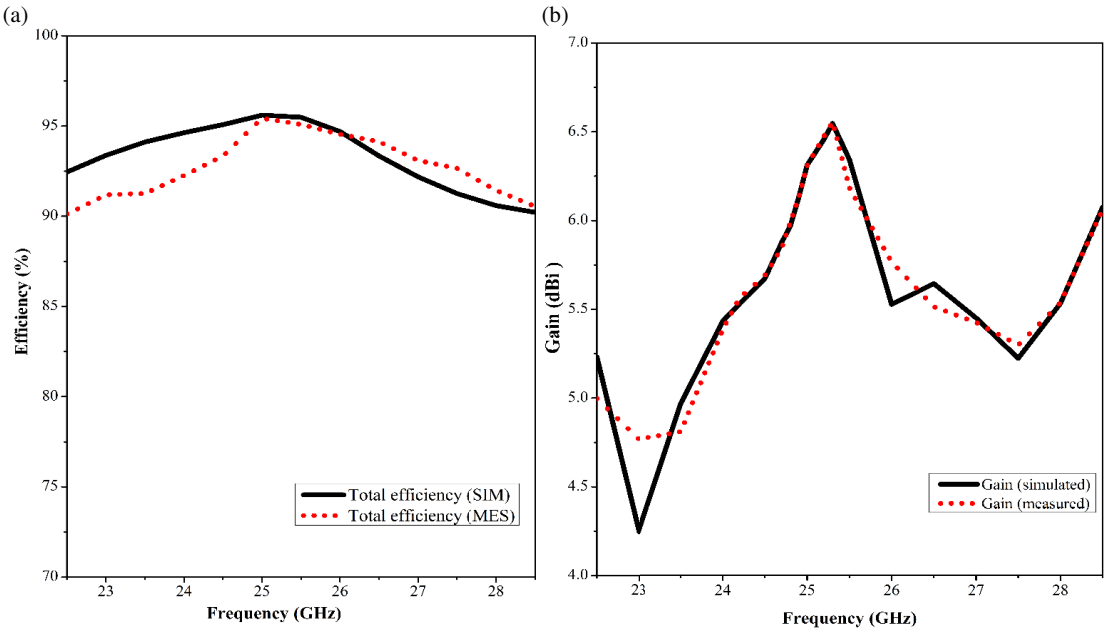

FIGURE 7. (a) Efficiency and (b) gain of the proposed MIMO antenna.

The primary means whereby decoupling is accomplished in our design is by carefully integrating elliptical and rectangular slots in the ground plane to create a Defected Ground Structure (DGS). This construction greatly reduces mutual coupling by limiting the surface current paths that would otherwise flow between adjacent antenna elements. Without the use of conventional decoupling networks, the DGS suppresses surface waves and redistributes current flow to achieve high isolation levels beyond 37 dB.

The decoupling is also influenced by the spatial arrangement and orientation of the elements. The overall MIMO performance is improved by utilizing polarization diversity and minimizing electromagnetic interaction through the strategic placement of the antenna elements with optimal spacing and alternate alignment.

The efficiency of the proposed MIMO antenna design is illustrated in Fig. 7(a). The overall efficiency of the MIMO antenna that has been proposed is 94.91% at the resonance frequency of 25 GHz. Fig. 7(b) displays the gain of the 5G MIMO antenna. The results unequivocally show the MIMO antenna having a maximum gain of 6.54 dBi and a resonant frequency gain of 6.3 dBi.

The surface current density pattern at a frequency of 25 GHz of the MIMO antenna is showcased in Fig. 8. Most of the current distribution is concentrated in the feedline and hook-shaped radiator. Since a single port is excited, and the other ports are terminated with a corresponding load of 50 ohms, slight surface currents are seen in the other ports.

Figures 9(a) and 9(b) show the co-polar and cross-polar radiation patterns in the E-plane (electric field) and H-plane (magnetic field), respectively. Exciting port one and terminating the other ports with a 50-ohm matched load yields the radiation patterns. In the E and H planes, the suggested MIMO antenna exhibits a directional radiation pattern. The symmetrical component layout of the MIMO configuration improves the 180-degree radiation pattern because the waves radiated by the individual antenna elements are coherently superposed.

Additionally, the DGS modifies the surface current distribution in specific ground plane regions. The observed directional radiation pattern is the result of constructive interference along a specified direction made possible by this current redirection. Mitigating surface waves attributable to the DGS inhibit the radiation in undesirable directions.

5. MIMO DIVERSITY PERFORMANCE

In the practical MIMO communication framework, to fully understand the prospects of the 8-element MIMO, the diversity performances are examined. The S-parameters procured for the MIMO antenna are used to determine the diversity performance metrics, namely the Diversity Gain (DG), Channel Capacity Loss (CCL), Mean Effective Gain (MEG), and Envelope Correlation Coefficient (ECC). As delineated in Equation (1), the ECC value measures the correlation between nearby antenna elements.

$$\rho_{ij} = \frac{|S_{ii}S_{ij} + S_{ji}S_{jj}|^2}{(1 - |S_{ii}|^2 - |S_{ij}{}^2|)(1 - |S_{jj}|^2 - |S_{ji}{}^2|)} \quad (1)$$

Fig. 10(a) depicts the graph for the suggested antenna's ECC. As is evident from the graph, the ECC value is less than 0.0003, which is very low, implying good diversity performance.

The DG of the suggested MIMO antenna is displayed in Fig. 10(b). As is ideal for any MIMO antenna, the DG's value is approximately 10 dB. Equation (2) mentions the formula that is used to calculate DG.

$$DG = 10\sqrt{1 - |ECC|^2} \quad (2)$$

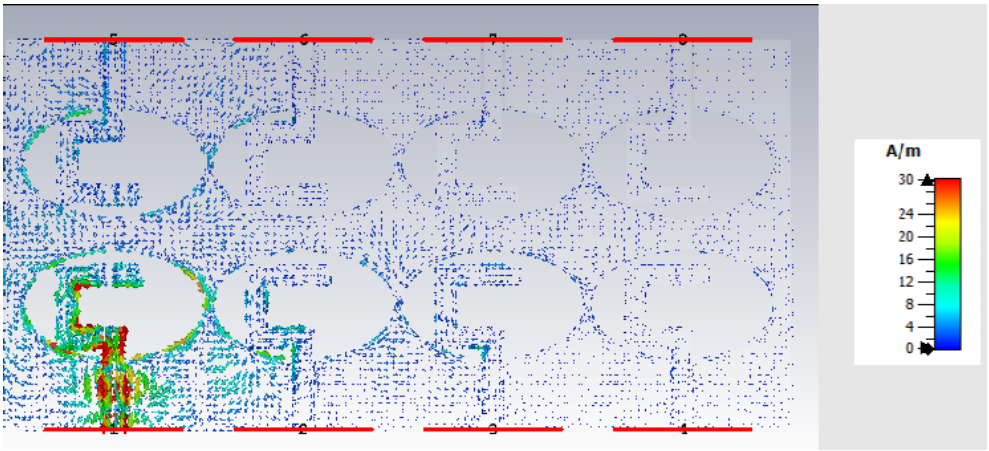

FIGURE 8. Suggested MIMO antenna's surface current distribution at 25 GHz.

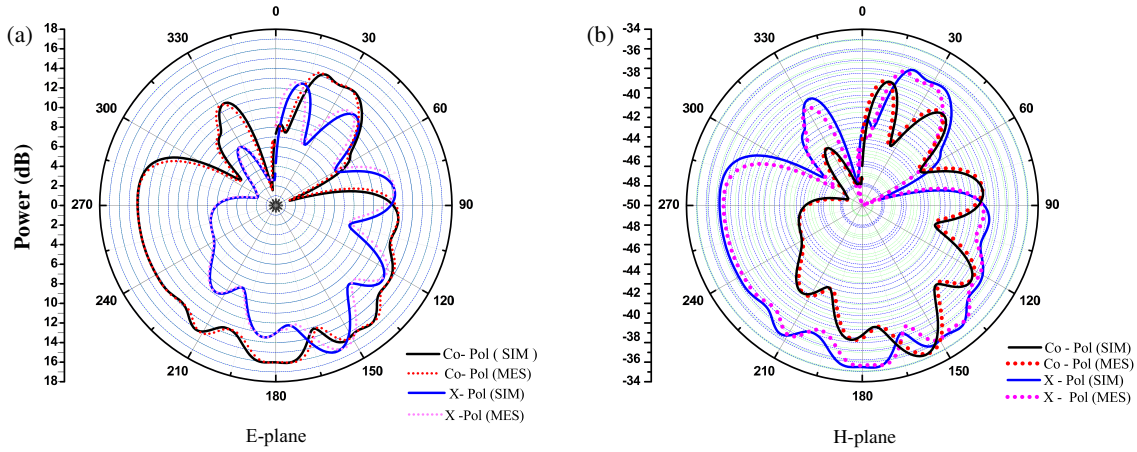

FIGURE 9. Radiation pattern of the suggested MIMO antenna design.

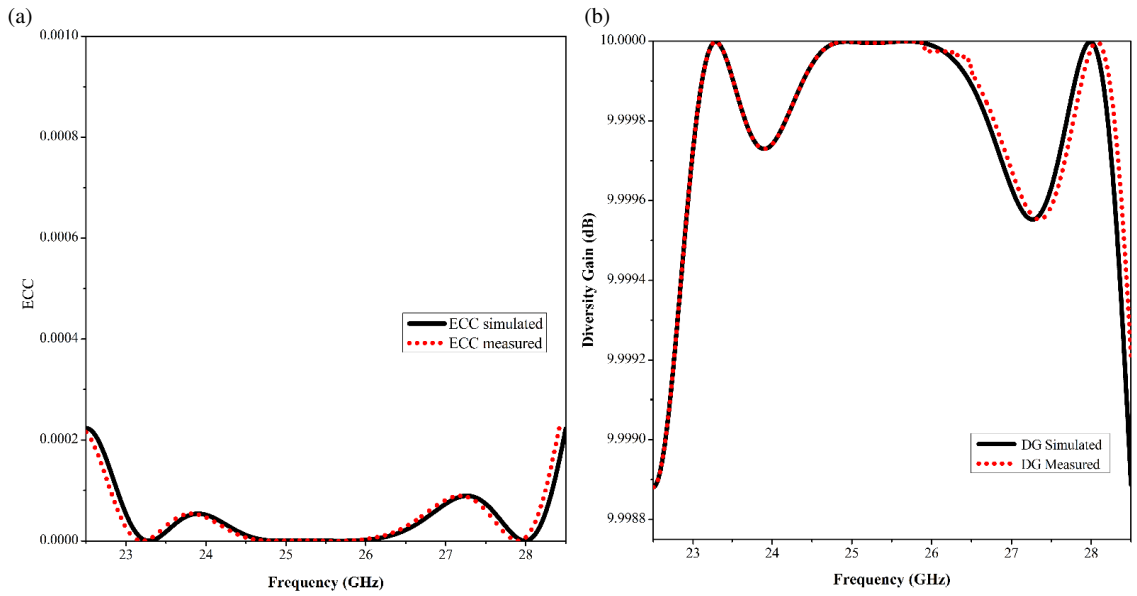

FIGURE 10. (a) ECC simulated and measured. (b) DG simulated and measured.

TABLE 3. Proposed MIMO antenna comparison with the previous literature.

Ref No.	No. of elements	Size (mm^2)	Antenna Type	Frequency (GHz)	Isolation (dB)	Isolation Technique	Efficiency (%)	ECC
[24]	2	19.94×15.06	Patch + EBG	24	-37	Electromagnetic band gap (EBG)	80.5	0.24
[25]	81	126×126	Antenna Array	24–29 30.5–36	-20	Antenna geometry	> 65	< 0.005
[26]	4	110×55	Patch + DGS	28/ 38	$-30/24$	Slots in ground	-	2.46×10^{-5} 7.65×10^{-5}
[27]	4	24×20	Optically Transparent Patch	24.10–27.18 33–44.13	-16	Full ground	75	$< 10^{-1}$
[28]	4	80×80	Circular Patch	23–40	> 10	Full ground	> 70	< 0.0014
[29]	4	150×70	Circular Patch + Parasitic Patches	4.776–5.052 22.7–28.5	$-32/-35$	-	60–65	-
[30]	10	100×40	Slot + DGS + DMS	22.5–28.5	-36.4	DGS and DMS (defective metal structure)	77	< 0.003
[31]	8	135×75	Transmission line (series fed)	27.5–31	-20	Stubs	-	< 0.015
[32]	4	12×45.2	GCPW-fed pentagonal patch + DGS	25.3–42	> 24	Defected ground structure (DGS)	> 82	< 0.0014
[33]	4	60.6×31.8	Antenna Array	28	> 30	Antenna orientation	91.5	< 0.00009
Proposed work	**8**	**62.7×31**	**Slot + DGS**	**22.5–27.5**	**< 37**	**DGS and antenna orientation**	**> 94**	**< 0.0003**

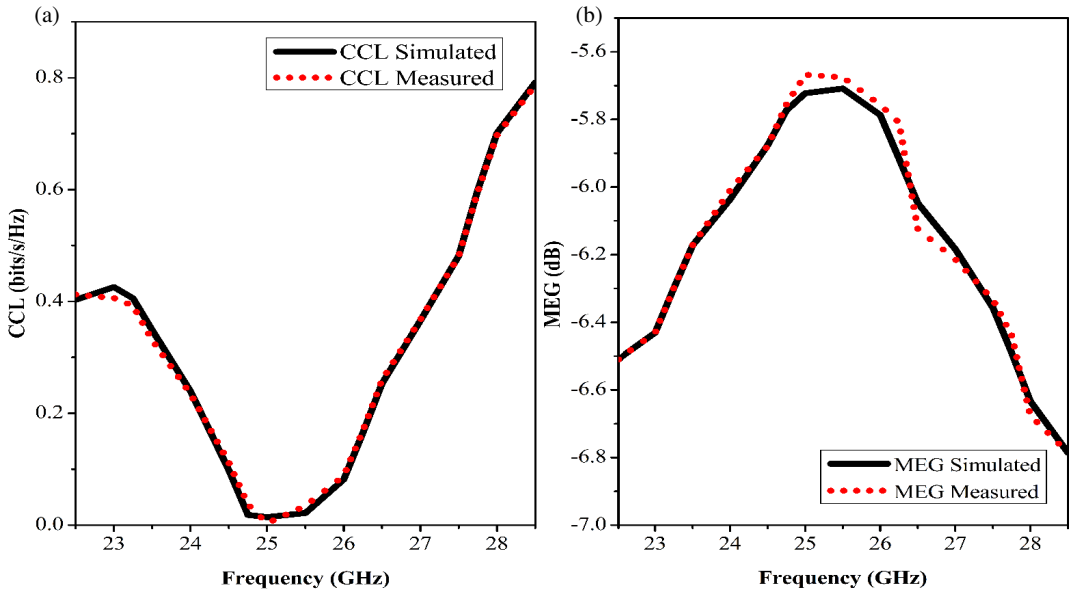

FIGURE 11. Simulated and measured results. (a) CCL. (b) MEG.

Channel capacity loss (CCL) can be calculated using the formula.

$$CCL = -\log_2 det[\beta^R] \tag{3}$$

where

$$[\beta^R] = \begin{bmatrix} \beta_{ii} & \beta_{ij} \\ \beta_{ji} & \beta_{jj} \end{bmatrix} \tag{4}$$

$$\beta_{ii} = 1 - \left(\sum_{j=1}^{N} |S_{ij}|^2 \right) \tag{5}$$

$$\beta_{ij} = -(S_{ii}^* S_{ij} + S_{ji}^* S_{ji}) \tag{6}$$

Channel capacity loss is shown in Fig. 11(a) and exhibits a value of 0.014 bits/s/Hz, and it is found to be less than 0.2, indicating that the proposed antenna has a reduced-loss data transmission.

Mean Effective Gain (MEG) denotes the mean power acquired by a wireless system functioning within a variable fading environment.

The MEG is given as

$$MEG = 0.5\mu_{ir} = 0.5\left[1 - \sum\nolimits_{j=1}^{l}(|S_{ij}|\right] \quad (7)$$

The computed and measured results for MEG are shown in Fig. 11(b). The permissible range for the MEG generally exists between -3 dB and -12 dB. Upon analysis of both the simulated and measured outcomes, it becomes apparent that the MEG value resides within the acceptable range. This observation highlights the relevance of the proposed study for MIMO and diversity-centric applications by demonstrating significant alignment between the simulated and measured performance metrics of the MIMO antenna design.

In Table 3, a comparison of the proposed MIMO antenna is made with the other designs studied from the literature [24–33]. The comparison is based on the antenna elements, design size, antenna type, isolation, and the technique used for isolation improvement. Additionally, the suggested antenna differs from the other larger designs due to its highly isolated elements, which have an isolation $<$ 37 dB. Without the need for any decoupling devices, the recommended antenna, however, offers a decent gain. Furthermore, the efficiency and ECC have been compared to the most recent studies, and the suggested design provides the highest efficiency and lowest ECC. Moreover, the majority of antennas have not looked at CCL and DG. The findings show that the suggested antenna is appropriate for millimeter-wave operations.

6. CONCLUSION

This article delineates a novel 8-element planar MIMO antenna tailored for the millimeter-wave 5G frequency band (n258) within a compact architectural framework. The antenna exhibits an exceptional efficiency rate of 94.9% alongside a peak gain of 6.3 dBi. DGS (Defected Ground Structure) configuration has been introduced to augment inter-element isolation, resulting in a high isolation level beyond 37 dB. It is noteworthy to highlight that, without using decoupling mechanisms, the achieved isolation remains significantly high. Indicative metrics of the performance of MIMO, like the Envelope Correlation Coefficient (ECC) and Diversity Gain (DG), show impressive values, with a DG of nearly 10 dB and an extraordinarily low ECC of less than 0.0003. The overall antenna architecture is characterized by its simplicity, devoid of intricate design complexities. All parameters associated with the antenna have been validated through empirical results, affirming the proposed antenna's viability for application in millimeter-wave 5G communication systems.

REFERENCES

[1] Dangi, R., P. Lalwani, G. Choudhary, I. You, and G. Pau, "Study and investigation on 5G technology: A systematic review," *Sensors*, Vol. 22, No. 1, 26, 2022.

[2] Ud Din, I., M. Alibakhshikenari, B. S. Virdee, R. K. R. Jayanthi, S. Ullah, S. Khan, C. H. See, L. Golunski, and S. Koziel, "Frequency-selective surface-based MIMO antenna array for 5G millimeter-wave applications," *Sensors*, Vol. 23, No. 15, 7009, 2023.

[3] Sokunbi, O., H. Attia, A. Hamza, A. Shamim, Y. Yu, and A. A. Kishk, "New self-isolated wideband MIMO antenna system for 5G mm-Wave applications using slot characteristics," *IEEE Open Journal of Antennas and Propagation*, Vol. 4, 81–90, 2023.

[4] Khan, A., Y. He, Z. He, and Z. N. Chen, "A compact quadruple-band circular polarized MIMO antenna with low mutual coupling," *IEEE Transactions on Circuits and Systems II: Express Briefs*, Vol. 70, No. 2, 501–505, Feb. 2023.

[5] Feng, Y., Y. Chen, and L. Cao, "A compact base station MIMO antenna array with miniaturized antenna elements," *IEEE Transactions on Circuits and Systems II: Express Briefs*, Vol. 71, No. 2, 607–611, Feb. 2024.

[6] Awan, W. A., E. M. Ali, M. S. Alzaidi, D. H. Elkamchouchi, F. N. Alsunaydih, F. Alsaleem, and K. Alhassoon, "Enhancing isolation performance of tilted Beam MIMO antenna for short-range millimeter wave applications," *Heliyon*, Vol. 9, No. 9, e19985, 2023.

[7] Sabek, A. R., W. A. E. Ali, and A. A. Ibrahim, "Minimally coupled two-element MIMO antenna with dual band (28/38 GHz) for 5G wireless communications," *Journal of Infrared, Millimeter, and Terahertz Waves*, Vol. 43, No. 3, 335–348, 2022.

[8] Munusami, C. and R. Venkatesan, "A compact boat shaped dual-band MIMO antenna with enhanced isolation for 5G/WLAN application," *IEEE Access*, Vol. 12, 11 631–11 641, 2024.

[9] Mohamed, H. A., M. Edries, M. A. Abdelghany, and A. A. Ibrahim, "Millimeter-wave antenna with gain improvement utilizing reflection FSS for 5G networks," *IEEE Access*, Vol. 10, 73 601–73 609, 2022.

[10] Saad, A. A. R. and H. A. Mohamed, "Printed millimeter-wave MIMO-based slot antenna arrays for 5G networks," *AEU — International Journal of Electronics and Communications*, Vol. 99, 59–69, 2019.

[11] Din, I. U., S. Ullah, N. Mufti, R. Ullah, B. Kamal, and R. Ullah, "Metamaterial-based highly isolated MIMO antenna system for 5G smartphone application," *International Journal of Communication Systems*, Vol. 36, No. 3, e5392, 2023.

[12] Esmail, B. A. F. and S. Koziel, "Design and optimization of metamaterial-based highly-isolated MIMO antenna with high gain and beam tilting ability for 5G millimeter wave applications," *Scientific Reports*, Vol. 14, No. 1, 3203, 2024.

[13] Shukoor, M. A., S. Dey, and S. K. Koul, "Review of metamaterial enabled electromagnetic absorbers for microwave to millimeter-wave applications," *IETE Technical Review*, Vol. 41, No. 6, 736–758, 2024.

[14] Parveez Shariff, B. G., A. A. Naik, T. Ali, P. R. Mane, R. M. David, S. Pathan, and J. Anguera, "High-isolation wide-band four-element MIMO antenna covering Ka-band for 5G wireless applications," *IEEE Access*, Vol. 11, 123 030–123 046, 2023.

[15] Khan, A., S. Bashir, S. Ghafoor, and K. K. Qureshi, "Mutual coupling reduction using ground stub and EBG in a compact wideband MIMO-antenna," *IEEE Access*, Vol. 9, 40 972–40 979, 2021.

[16] Sufian, M. A., N. Hussain, A. Abbas, J. Lee, S. G. Park, and N. Kim, "Mutual coupling reduction of a circularly polarized MIMO antenna using parasitic elements and DGS for V2X communications," *IEEE Access*, Vol. 10, 56 388–56 400, 2022.

[17] Sakli, H., C. Abdelhamid, C. Essid, and N. Sakli, "Metamaterial-based antenna performance enhancement for MIMO system applications," *IEEE Access*, Vol. 9, 38 546–38 556, 2021.

[18] Taher, F., H. A. Hamadi, M. S. Alzaidi, H. Alhumyani, D. H. Elkamchouchi, Y. H. Elkamshoushy, M. T. Haweel, M. F. A. Sree, and S. Y. A. Fatah, "Design and analysis of circular polarized two-port MIMO antennas with various antenna element orientations," *Micromachines*, Vol. 14, No. 2, 380, 2023.

[19] Elalaouy, O., M. E. Ghzaoui, and J. Foshi, "A high-isolated wideband two-port MIMO antenna for 5G millimeter-wave applications," *Results in Engineering*, Vol. 23, 102466, 2024.

[20] Ghosh, S., G. S. Baghel, and M. Swati, "Design of a highly-isolated, high-gain, compact 4-port MIMO antenna loaded with CSRR and DGS for millimeter wave 5G communications," *AEU — International Journal of Electronics and Communications*, Vol. 169, 154721, 2023.

[21] Sghaier, N., A. Belkadi, M. A. Malleh, L. Latrach, I. B. Hassine, and A. Gharsallah, "Design and analysis of a compact MIMO antenna for 5G mmWave N257, N260, and N262 band applications," *Journal of Infrared, Millimeter, and Terahertz Waves*, Vol. 45, No. 3, 247–264, 2024.

[22] Güler, C. and S. E. B. Keskin, "A novel high isolation 4-port compact MIMO antenna with DGS for 5G applications," *Micromachines*, Vol. 14, No. 7, 1309, 2023.

[23] Singh, A. K., S. K. Mahto, and R. Sinha, "Compact super-wideband MIMO antenna with improved isolation for wireless communications," *Frequenz*, Vol. 75, No. 9-10, 407–417, 2021.

[24] Iqbal, A., A. Basir, A. Smida, N. K. Mallat, I. Elfergani, J. Rodriguez, and S. Kim, "Electromagnetic bandgap backed millimeter-wave MIMO antenna for wearable applications," *IEEE Access*, Vol. 7, 111 135–111 144, 2019.

[25] Wang, F., Z. Duan, X. Wang, Q. Zhou, and Y. Gong, "High isolation millimeter-wave wideband MIMO antenna for 5G communication," *International Journal of Antennas and Propagation*, Vol. 2019, No. 1, 4283010, 2019.

[26] Marzouk, H. M., M. I. Ahmed, and A. Shaalan, "Novel dual-band 28/38 GHz MIMO antennas for 5G mobile applications," *Progress In Electromagnetics Research C*, Vol. 93, 103–117, 2019.

[27] Desai, A., C. D. Bui, J. Patel, T. Upadhyaya, G. Byun, and T. K. Nguyen, "Compact wideband four element optically transparent MIMO antenna for mm-wave 5G applications," *IEEE Access*, Vol. 8, 194 206–194 217, 2020.

[28] Sehrai, D. A., M. Abdullah, A. Altaf, S. H. Kiani, F. Muhammad, M. Tufail, M. Irfan, A. Glowacz, and S. Rahman, "A novel high gain wideband MIMO antenna for 5G millimeter wave applications," *Electronics*, Vol. 9, No. 6, 1031, 2020.

[29] Sharma, S. and M. Arora, "A millimeter wave elliptical slot circular patch MIMO antenna for future 5G mobile communication networks," *Progress In Electromagnetics Research M*, Vol. 110, 235–247, 2022.

[30] Nej, S., A. Ghosh, S. Ahmad, J. Kumar, A. Ghaffar, and M. I. Hussein, "Design and characterization of 10-elements MIMO antenna with improved isolation and radiation characteristics for mm-Wave 5G applications," *IEEE Access*, Vol. 10, 125 086–125 101, 2022.

[31] El-Nady, S. M. and A. M. Attiya, "Periodically-stub-loaded microstrip line wideband circularly polarized millimeter wave MIMO antenna," *IEEE Access*, Vol. 10, 20 465–20 472, 2022.

[32] Kumar, A., A. Kumar, and A. Kumar, "Defected ground structure based high gain, wideband and high diversity performance quad-element MIMO antenna array for 5G millimeter-wave communication," *Progress In Electromagnetics Research B*, Vol. 101, 1–16, 2023.

[33] Sehrai, D. A., M. E. Munir, S. H. Kiani, N. Shoaib, A. D. Algarni, H. Elmannai, M. M. Nasralla, and T. Ali, "A high gain array based millimeter wave MIMO antenna with improved isolation and decorrelated fields," *IEEE Access*, Vol. 12, 89 794–89 803, 2024.